Green Chemistry

Accepted Manuscript

ROYAL SOCIETY OF CHEMISTRY

www.rsc.org/greenchem

Thermo-compression molding of chitosan with deep eutectic mixture for biofilms development

Andrea C. Galvis-Sánchez[a,*], *Ana M. M. Sousa*[a,b], *Loic Hilliou*[c], *Maria P. Gonçalves*[a], *Hiléia K.S. Souza*[a,*]

[a] REQUIMTE/LAQV, Departamento de Engenharia Química, Faculdade de Engenharia, Universidade do Porto, Rua Dr. Roberto Frias, 4200-465 Porto, Portugal.

[b] Agricultural Research Service, U.S. Department of Agriculture, Eastern Regional Research Center, Dairy & Functional Foods Research Unit, 600 East Mermaid Lane, Wyndmoor, PA 19038, USA.

[c] Institute for Polymers and Composites/I3N, University of Minho, Campus de Azurém, 4800-058 Guimarães, Portugal.

Corresponding Authors

*Andrea C. Galvis-Sánchez (Phone: +351 220414838; E-mail address: asanchez@fe.up.pt); Hiléia K. S. Souza (Phone: +351 220414838; E-mail address: hsouza@fe.up.pt)

Abstract

Eutectic mixture of choline chloride (ChCl) and citric acid (CA) were successfully used for the preparation of chitosan (Chit) bio-films by thermo-compression molding. Optimization of the film preparation condition was carried out using response surface methodology and Box-Behnken design based on the best mechanical properties and lowest energetic requirements (lower compression load and time). The optimum film made with chitosan and ChCl-CA (eutectic mixture) was compared with films prepared using only CA in their formulation. Chit-ChCl-CA films presented higher elasticity, opacity, total color difference and lower tensile strength in relation to the Chit-CA films. Films prepared with the eutectic mixture presented higher water vapor permeability values. These results were associated with films microstructures. FTIR analysis confirms the occurrence of chemical changes in the processed films. The thermo-compression process affects significantly the crystallinity of the pristine chitosan. Films thermal stability is depressed when compared to the stability of each component.

Introduction

Growing concerns on the environmental impact of non-biodegradable oil-derived plastics is triggering the exploration of more sustainable alternatives. In this respect, the development of scalable manufacturing processes exploiting biomass resources is getting increasingly popular. Polysaccharides (Pls) are certainly one of the best candidates to serve in biofabrication as they are an abundant, biodegradable and greatly biocompatible. In this sense, starch, cellulose, and chitosan are the main Pls used for the manufacture of bioplastics as alternative materials for e.g. food packages and other applications.[1]

Chitosan (Chit), a natural polysaccharide obtained by deacetylation of chitin which is an abundant component in the exoskeletons of crustaceans such as crabs, lobsters, and shrimps, has been intensively studied in the preparation of bioplastics and/or biofilms for food packaging applications. In the latter case, in spite of the good film transparency usually achieved, poor mechanical properties and great moisture sensitivity limit the development of commercial products.[2] Some approaches to improve films' properties included the addition of plasticizers, the use of chemically-modified chitosans, and others; but they either introduced poorly biodegradable (or toxic) compounds or led to poorer mechanical properties.[3,4]

The functionalities of Chit films are known to depend on several factors including polysaccharide structure and properties (chitosan molecular mass and degree of deacetylation), type of organic acid used for Chit solubilisation, film composition, plasticizer type and concentration, and fabrication process.5 For instance, Souza et al., 2013[6] recently reported the effect of Chit molecular mass on the morphology of Chit nanoparticles (NPs) biofilms without plasticizer. The authors demonstrated that the mechanical properties of the biofilms made from material mostly composed of colloidal microfibers and spherical NPs turned increasingly poorer. Interestingly, the lowest water permeability was exhibited by the films prepared from the NPs chitosan, suggesting that the high surface areas and surface-to-volume ratios characterizing the nanoparticulated systems may provide a physical barrier to water molecules. Regarding the introduction of additives, the effect of plasticizer type on films' characteristics has been extensively studied as plasticizer has a significant influence on the stability of films properties during storage and applications.[7]

In an effort to find alternative and sustainable solvents to replace current organic solvents used for common chemical processing operations, a new alternative approach of "environmentally friendly solvents and benign reaction media" is required

in order to comply with the *Green Chemistry* principles. In this context eutectic mixtures have emerged with promising results.[8,9] Eutectic mixtures are obtained by mixing two cheap and safe solid components that are capable of self-association, often through hydrogen bond interactions, forming a eutectic mixture with a melting point lower than that of each individual component.[10] Among the most promising applications, eutectic mixtures based on choline chloride (ChCl) and a hydrogen bond donors like urea or glycerol were reported to work as functional additives for biofilms preparation.[11,12,13,14] Abbott *et al.,* 2012[11] used eutectic mixture (ChCl/urea) for production of thermoplastic corn starch film. In this sense, the incorporation of the eutectic mixture leads stronger, more flexible films when compared with films containing only urea. Sousa *et al.,* 2014[14] studied the effect of deep eutectic solvents (DES) mixtures (ChCl/urea and ChCl/glycerol) in the fabrication of non-aqueous agar biofilms. The results showed that, even in the range of low polymer concentrations used, commercial agar/DES (ChCl/Urea) system showed good film-forming ability exhibiting good mechanical resistance and enhanced flexibility when compared with typical aqueous agar films.

Furthermore, the combination of ChCl with other biodegradable and non-toxic components like organic acids, sugars, polyalcohols, amines and amino acids were also reported as possible candidates for the preparation of eutetic mixtures.[9] But the use of ChCl-based eutectic mixtures as processing aids for the production of Chit biofilms has not yet been reported.

Here, we present an innovative and, to the best of our knowledge, unexplored approach based on the use of environmentally friendly low-melting mixtures recently referred to as Deep Eutectic Solvents (DESs)[9] which are expected to play the role of functional additive for the production of chitosan biofilm. The natural eutectic mixture of ChCl-citric acid is used as precursor for the fabrication of chitosan transparent films by thermo-compression molding. Formulation was optimized for best mechanical properties, namely best tensile strength and elongation at break. The effect of the selected eutectic mixture on the processed films was evaluated by assessing the mechanical, water resistance, microstructure and thermal properties of the films at optimized processing conditions. The impact of compression molding parameters on films mechanical properties was also studied.

Materials and methods

Materials

Commercial sample of chitosan, ChitoClear,® batch number TM2791, was purchased to Primex (Siglufjordur, Iceland). This product is extracted from shrimp shells from the North Atlantic Ocean and further de-acetylated to a degree of 90% (DD=90%). Although, according to the supplier, the average molecular mass (M) falls in the range 250-300 kDa, viscosimetric measurements have shown that the viscosity-average molecular mass (MV) is higher: over 650 kDa in acetate buffer pH 6[6] and over 330 kDa in acetate buffer pH 4.7[15]. Hereinafter, we will refer to this high-M chitosan as CHIT90. Previous research conducted by our group has also elucidated its great degree of polydispersity in terms of colloidal size. Accordingly, the morphological inspection of CHIT90 through AFM and SEM allowed identifying the coexistence of polymer-like microfibers packed with nanoparticles of small (10-30 nm) and medium (150-300 nm) size[6]. Using Dynamic Light Scattering technique, the chitosan was also characterized by a high degree of polydispersity what is well supported by the high polydispersity index derived from the mathematical analysis of the data (PdI=3).

Choline chloride (Sigma, molecular weight = 139.62 g/mol, purity approx. 99%) and citric acid-1-hydrate (Panreac, molecular weight = 210.14 g/mol, purity approx. 99%) were used as received. An acetic acid solution at 3% (v/v) was prepared using glacial acetic acid (Merck, purity: >99%) and sodium hydroxide solution (0.1 mol/L) was prepared using sodium hydroxide (AnalaR Normapur, molecular weight = 40.0 g/mol). Deionized water was used throughout experiments.

Sample preparation

Chitosan (Chit) films were prepared according to the method described by Abbott *et al.,* 2012[11] and Matet *et al.,* 2013[16]. Chit and choline chloride (ChCl) were first dried in an oven for at least 24 h at 70 ^{o}C before use. Then, the three powders Chit, ChCl and citric acid (CA) were mixed for 15 min using pestle and mortar in amounts specified by an experimental design approach (Table S1 and Figure 1). The ratio ChCl and CA was set at 1:1 to ensure the formation of the natural eutectic mixture. The whole mixture was then placed in oven at 70 ^{o}C for 30 min. The hot paste was removed from the oven and subsequently, the aqueous acetic acid solution (3% w/w) was slowly added and manually mixed during 15 min. The chitosan/acetic acid solution ratio was kept constant for all the formulations at 25/75 (wt/wt). Finally, the resulting materials were hot-pressed as describe bellow.

In addition, a formulation of Chit and citric acid (CA) was also tested using the optimum condition (after optimization strategy, see ESI). The procedure for preparing this formulation was the same as described above for Chit and the eutectic mixture (ChCl and CA, 1:1). For simplification, the shorthand notation Chit-ChCl-CA and Chit-CA was adopted along the manuscript for the designation of chitosan film prepared using the eutectic mixture (ChCl-CA) and for the film formed just with CA, respectively.

Film fabrication

Approximately 1g of the paste prepared as described above was placed in a circular mold (diameter = 5cm and thickness = 2 mm). Then, the filled mold was placed between two stainless steel plates covered with aluminum foil, the circular mold was removed before compression molding, and the paste was hot press-molded using a hydraulic press (Carver laboratory press, model 3856CE, Fred S. Carver Inc., New Jersey, USA).

Film samples were prepared at various sets of conditions of eutectic mixture percentage, compression load and compression time (Table S1). The compression temperature was fixed at 120 °C since higher and/or lower temperatures would consistently lead to respectively, polymer degradation or no film is formed. All prepared films were stored at 53% relative humidity (R.H.) and 25 ^{o}C for at least 48 h before their characterization.

Optimization strategy

The optimization strategy combined the use of a three-level-three-factor Box-Behnken design (BBD) with response surface methodology (RSM).[17] More details about films processing optimization can been seen in the ESI.

Characterization of films

Scanning electron microscopy (SEM)

SEM images were acquired in the secondary electron mode using an FEI Quanta 400 FEG microscope located at CEMUP (Centro de Materiais da Universidade do Porto). Samples were previously cryo-fractured using liquid N_2 and mounted on aluminium stubs covered with double-coated carbon conductive adhesive tabs. Afterwards, the samples were coated with a thin film of Au/Pb and imaged in the high-vacuum/secondary electron imaging mode using an accelerating voltage of 5 kV and the working distances oscillated between 10.4 to 13.8 mm.

Thickness measurements

The thickness of the films was measured to the nearest 0.001 mm using a digimatic indicator (Model, ID-F150, Mitutoyo, Aurora, IL, USA). At least, five measurements at different positions were performed for each film.

Mechanical properties

The mechanical properties (tensile strength, *TS*; Young's modulus, *YM* and elongation at break, *E*) of the films were measured using a texture analyser (Model TA-XT2, Stable Micro Systems Ltd, Surrey, UK) equipped with the Stable Micro Systems XT.RA Dimension data acquisition software. Film samples with dimensions of 25 mm x 100 mm were cut from produced films for tensile testing. A 12 mm/min strain rate and a gauge length of 80 mm were the conditions used in all experiments. At least five replicates were performed for each film formulation.

Sorption isotherms

Water sorption isotherms were determined gravimetrically as described by Larotonda, 2007 and Sousa, 2014.[18,14] Film samples with dimensions of approximately 25 mm x 25 mm, were previously dried under vacuum at 60 ^{o}C for 48 h. After that, samples were placed into hermetic containers with equilibrium water activities (a_w) ranging from 0.11 to 0.90 at room temperature. The samples were periodically weighted until achieving a constant value. The water sorption isotherm of a material is defined as the relation between the equilibrium water activity and the corresponding moisture content (dry basis) of the sample at a given temperature. Several models have been proposed to fit the water sorption data and provide additional thermodynamic information about the studied systems.[14] In this study the Guggenheim–Anderson–de Boer (GAB) equation Eq. (1), was used to fit the experimental sorption data,

$$X_e = (C \cdot k \cdot X_0 \cdot a_W) / ([1-k \cdot a_W] \cdot [1-k \cdot a_W + C \cdot k \cdot a_W]) \quad (1)$$

Where, X_0 represents the monolayer moisture content, also on dry basis, C is a constant dependent on the water sorption heat in the first layer and subsequent layers and k is a parameter reflecting the sorption heat of the multilayer as well as the heat of condensation of water vapor. Duplicate measurements were performed for each optimum film formulation.

Water vapor permeability (WVP)

Permeability tests were conducted by following the Standard Test Method for Water Vapor Transmission of Materials (ASTM E96-00, 2000).[19] The procedure for WVP was previously described by Larotonda (2007).[18] In this case, film samples of 80 mm in diameter were tightly sealed to a permeation cell containing calcium chloride (RH = 2%). The cells were placed in a desiccator filled with water (RH = 100%) and equipped with a fan that promotes the air convection and facilitates water diffusion. The cell was periodically weighted and the WVP in g m^{-1} s^{-1} Pa^{-1} was obtained from Eq. 2.

$$WVP=(\Delta m \cdot x) / (A \cdot \Delta t \cdot \Delta P) \quad (2)$$

Where Δm is the weight gain (g), x is the film thickness (m), and A is the area (0.003 m^2) exposed for a time Δt (s) to a partial water vapor pressure Δp (Pa).

Optical properties

Total color difference (*Delta E*) and opacity were determined with a hand-held tristimulus reflectance colorimeter (Model CR-300, Minolta, Japan). A white standard color plate (Y = 92.7, x = 0.3133, y = 0.3194) was used as a background for color measurements. *Delta E* was recorded using a CIE L*a*b* system and calculated using the Eq. (3), where L*, a*, and b* represent the standard values of the white calibration plate used as a background during film's measurements.

$$\text{Delta E} = \sqrt[2]{(L-L*)^2 + (L-L*)^2 + (L-L*)^2} \quad \text{Eq. (3)}$$

The opacity of a material is an indication of how much light passes through it; the higher the opacity the lower the amount of light that can pass through the material. The opacity of the samples was determined using the Eq. (4), as the relationship between the opacity of each sample on a black standard (Y_b) and the opacity of each sample on the white standard (Y_w). Both *Delta E* and opacity parameters were measured five times at different places in each film specimen.

$$Opacity\ (\%) = Y_b/Y_w \,.\, 100 \quad (\text{Eq. } 4)$$

Fourier transform infrared spectroscopy (FTIR)

All FTIR spectra were acquired using a spectrometer (Spectrum 100, PerkinElmer Ltd) equipped with a Diffuse Reflectance Sampling Accessory (DRIFT). Films produced at the optimum selected conditions were cut to produce samples of approximately 1cm x 1cm, and scratched onto the abrasive pad of the DRIFT accessory. FTIR spectrum of powdered chitosan was also acquired using the same accessory, pouring directly a small amount of powder onto the pad. All spectra were registered between 4000–600 cm^{-1}, and collected at a resolution of 2 cm^{-1}; 16 scans were averaged before Fourier transformation.

In order to evaluate the possible cross-linking effect between CA and Chit a procedure was performed based on experiment reported by de Cuadro *et al.,* 2015.[20] Chit-ChCl-CA and Chit-CA films produced at the optimum selected conditions were cut and immersed in an aqueous solution of NaOH (0.1 mol/L) for 2 min at room temperature. Then, the samples were removed, dried and spectral acquisition was performed.

Thermogravimetric analysis (TGA)

TGA thermograms of films and films components were obtained using a TA Q500 (TA Instruments). Each film sample or powder (typically 15 mg) was placed in the TGA furnace and heated from 30 ^{o}C to 60 ºC. A 20 minutes rest time at this temperature allowed for the removal of the residual water bounded to samples, and samples were heated up to 300 ^{o}C at a heating rate of 10 ^{o}C/min under nitrogen atmosphere.

Differential Scanning Calorimetry (DSC)

Thermal properties of films were studied using a differential scanning calorimeter (Diamond Pyris, PerkinElmer Ltd.). Each film sample (approximately 5 mg) was equilibrated at -30 ºC during 10 minutes and heated from -30 ºC to 200 ^{o}C at 10 ^{o}C/min (first heating run), then cooled down to -20 ºC at a rate of -10 ºC/minute and finally heated up to 200 ºC (second heating run) at a rate of 10 ºC/min. All heating and cooling runs were performed under nitrogen atmosphere. From the thermograms, the following parameters were obtained: onset and melting temperatures and melting enthalpy.

Other Statistical Analysis

Statistica version 8.0 software was used for other statistical analyses. Differences between means of other film properties were examined using the Student's *t*-test and

were considered significant at $p<0.05$. A non-linear estimation was used to fit the experimental sorption data to Eq. (1) and obtain the correspondent GAB parameters.

Results and discussion

Optimal conditions for film production

The optimization strategy for film production is detailed in the ESI. The output of the optimization is the following set of parameters for film production: 30% plasticizer, 176.5 kN, 10 min (see ESI).

Films morphology and structure

Cross sections of the cryo-fractured Chit-ChCl-CA and Chit-CA are presented in Figs. 2D and 2E, respectively. Both pictures are overall similar, only fracture zones are seen and otherwise the section is homogenous. Chit-CA shows a sheet-like pattern structure without fractured zones, which is expected from mechanical characteristics since it is more brittle and thus will break more easily during cryo-fracture (Fig. 2E). No phase separation between Chit and CA neither between Chit and the eutectic mixture (ChCl-CA) was seen in the cross-sections of fractured films, at least at over the length scaled probed in Figs. 2D and 2E (1000x magnification). Images of films surfaces (see Fig 2A for Chit-ChCl-CA film and Fig. 2B for Chit-CA film) presented some non-homogenous domains, but this could come from the molding and demolding process (surface effects), not from the intrinsic structure of the films. A previous study demonstrated that the type of acid and the concentration of chitosan used for film preparation can affect the spatial configuration of the chitosan molecules during film formation.[21] It was shown that the use of acetic acid as dissolved solution and its interaction with the citric acid promoted the reorganization of chitosan molecules. Indeed, Figs. 2C and 2F show that Chit films prepared with ChCl-CA without acetic acid presented a heterogeneous microstructure with voids. This suggests that sintering of Chit-ChCl-CA grains occurred during compression molding, in contrast to films formulated with acetic acid.

X-ray diffraction (XRD) analyses were performed to determine the influence of the processing method and of the use of eutectic mixture using ChCl and citric acid on the crystalline structure of the chitosan films. The X-ray diffraction patterns of chitosan powder (as received), Chit-ChCl-CA and Chit-CA films are compared in Fig. S2 (ESI). The WAXD spectrum of the powdered chitosan resembles the chitosan spectrum presented by Matet *et al.,* 2013[16], showing the presence of crystalline regions with two main peaks at 10^{o} and at 20^{o}. The peak at 10^{o} is assigned to the

hydrated crystals due to the integration of water molecules in the crystal lattice and the peak located at 20° is associated with the most ordered regions attributed to the regular crystal lattice of chitosan.[22] However, these broad peaks sit on a large amorphous hallow indicating that the powder is essentially amorphous.

WAXD of compressed molded films exhibit a reduction in the crystallinity of the chitosan component, in comparison with its powder form. Indeed, the peak at 10° is just buried in the noise, whereas a drastic decrease in the intensity of the peak at 20° is observed Fig. S2 (ESI). Overall both types of films show similar residual crystallinity attributed to the modifications of the crystalline structure of chitosan due to processing conditions at 120 ºC.

Differential scanning calorimetry (DSC)

To further understand the structure and the effect of components (ChCl-CA and CA) on chitosan films' properties, DSC study of processed films was performed. The first heating runs are displayed in Fig. 3a, whereas the second heating runs after cooling (the cooling runs were featureless for the two types of films) are presented in Figure 3b.

Regarding the first heating, the calorimetric curves obtained for Chit-ChCl-CA film are characterized by two processes (Fig. 3a). The first broad thermal process for Chit-ChCl-CA film was around 90 °C and can be related to the loss of water.[7] Note that the latter is less pronounced in the DSC curve of Chit-CA, which is expected as much less water is present in this film (see TGA and water sorption data). The second thermal process for Chit-ChCl-CA film stating at around 150 ºC is reminiscent from the thermal process exhibited by the Chit-CA film for temperatures above 170 °C. However the end of this thermal process falls out of the temperature window explored in Fig 3. Thus it is not possible to assign this process to a glass transition or a melting of crystals. Nevertheless, WAXD data suggested that films were essentially amorphous. We thus conjecture that this process corresponds to a glass transition. In the literature, such event is usually related to the glass transition temperature (T_g) of chitosan. In this sense, various T_g values were determined for chitosan by DSC and were reported to be between 103 °C to 203 °C.[7,23,24] Building on such interpretation together with the amorphous nature of films assessed by WAXD, Fig 3 shows that the T_g for Chit-ChCl-CA occurs at a lower temperature than for Chit-CA. This indicates that the eutectic mixture is a better plasticizer of chitosan.

The second heating run recorded with the two films is essentially similar as no thermal process is seen in the range of temperatures tested (Fig. 3b). As such, the second heating is critically different from the first one, as no process at 90 ºC or at

177-185 ºC is resolved. However, a small peak located at 26 ºC is observed for Chit-ChCl-CA films, indicating a weak process (Fig. 3b). Note that this small process also shows up at the same temperature during the first heating run (Fig. 3a). As such, this peak relates to a thermally reversible process. The fact that such process is absent in Chit-CA film suggests that it relates to ChCl or to the eutectic component.

TGA data (see below Figure 6) suggest that the onset for thermal degradation occurs at nearly 170 ºC for the two films. In addition, TGA curves of both films are similar. Thus, partial degradation of ChCl/CA occurred during the first DSC heating of films. However, it cannot explain the differences in the thermal properties of the two films, nor the differences between the two heating runs of a sample. Rather, the thermomechanical history of the film forming process which has been erased during the first heating better explains such differences.

Water sorption studies and water vapor permeability

Moisture sorption studies were performed at 25 ^{o}C and used to evaluate the moisture sensitivity of Chit-ChCl-CA and Chit-CA films over a wide range of a_w. This information permits a better insight of the water sorption phenomenon at the primary sites of the polymeric material when equilibrium is reached, as well as energetic requirements related to differences in the chemical potential of water molecules at the monolayer and upper layers.[14]

Experimental data was fitted using the GAB equation Eq. (1). The GAB estimated parameters are listed in Table 1 and the respective fittings are represented in the Fig. 4. The moisture content increased for the two film samples by increasing a_w, following in both cases a sigmoid shape Fig. 4. Quantitative information derived by fitting the data to the GAB model (Eq. 1) shows that good correlation coefficients were obtained ($R^2 > 0.98$) in all cases and k values ($0 < k < 1$) suggested that the model adequately fit the experimental data (Table 1).[14]

The amount of water retained at the primary sorption sites of the polymeric film was quantified on a dry basis by X_o (Table 1). In general, the values for this parameter were very low for the two film samples in comparison with the values reported for chitosan biofilms (0.047 – 0.166) produced by knife coating method[6], suggesting a decline in the water uptake capacity of the produced films at equilibrium conditions.

C is a function of the energy difference between adsorption in the form of one monolayer and/or in several multilayers. C values of the two film formulations were higher (Table 1) than values reported for chitosan biofilms prepared by knife-coating technique (1.7 – 4.3).[6] In this case, high C values could reflect that adsorption of

water by these films were characterized by a monolayer of molecules strongly bounded to the material; especially for Chit-ChCl-CA films (*C* = 6.65) in comparison with Chit-CA films (*C* = 6.15). Also, this high *C* value could indicate that subsequent molecules were only slightly or were not structured in the upper layers.

Water vapor permeability (WVP) of the films can depend on different factors those including chitosan molecular weight, type and concentration of plasticizer, film preparation technique, method used for WVP determination, among others.[25] In this case Chit-ChCl-CA films presented higher WVP value than Chit-CA films (Table 1). WVP value of Chit-ChCl-CA films was in the range of the WVP values reported for films prepared using chitosan with different molecular weights and different organic acids (2.6 to 6.9 x 10^{-10} g m^{-1} s^{-1} Pa^{-1}).[25] On the other hand, WVP value of Chit-CA films was lower than the values found for chitosan casting films prepared using organic acids.[25] According to the SEM results (Figs. 2A and B) it might be possible to infer that Chit-ChCl-CA films could present a wide interstitial space (higher free volume) allowing a greater diffusion rate of water molecules. The interaction between the polysaccharide and the eutectic mixture, ChCl-CA, could permit the formation of small interstitial spaces between the polymeric structure permitting that at least one of the permeation processes can occur (*i.e.* absorption, diffusion and desorption). Taking in consideration the water sorption studies it is possible to admit that the absorption of water molecules was thermodynamically favored yet its diffusion and desorption were slower as the Chit-ChCl-CA films were characterized by a monolayer of molecules strongly bounded to the material according with the interpretation of the values of the *C* parameter (Table 1). So, it might be possible to assume that the water molecules more strongly bonded to the polymer structure will need longer times to diffuse and desorb from the polymeric structure.

Fourier transform infrared spectroscopy (FTIR)

FTIR analysis of films samples was performed in order to better understand the effect of compression molding process on the chemistry of the films. Fig. 5a shows FTIR spectra bands corresponding to the chitosan powder, the Chit-CA and the Chit-ChCl-CA films.

The Chit-CA spectrum shows spectral bands characteristic of the chitosan powder, with a broad band at 3600 to 3000 cm^{-1} and centered at around 3400 cm^{-1} corresponding to the O–H and N–H stretching vibrations; and two small peaks at 2935 and 2894 cm^{-1} corresponding to C-H stretching bands.[16] The amide I band present in pure chitosan powder at 1660 cm^{-1} was at 1650 cm^{-1} in the Chit-CA spectrum film. The bending absorption band of N–H in amide II at 1555 cm^{-1} in pure

chitosan was at 1560 cm^{-1} in the Chit-CA spectrum film. More, the small band intensity at 1376 cm^{-1} (of C–N in amide III) in the pure chitosan presented a more intensive band at 1381 cm^{-1} in the film. Furthermore, C–O stretching bands at 1150 (anti-symmetric stretching of the C–O–C bridge); and the 1084 and 1050 cm^{-1} (skeletal vibrations involving the C–O–C stretching) in pure chitosan were displayed at 1155, 1070 and 1024 cm^{-1} in the Chit-CA film. An absorption band at 895 cm^{-1} in the chitosan, corresponding the C–O–C bridge as well as glucosidic linkage was also observed in the Chit-CA film.[26] Other absorption bands were also observed in the Chit-CA film; the characteristic band of acetate group (C=O) of acetic acid at 1704 cm^{-1} and because of the interaction between the $–COO^-$ in the acetic acid and the NH_3^+ in chitosan a small shoulder at 1530 cm^{-1} was also observed.[27,16]

Chit-ChCl-CA film presented similar spectral bands to those observed in Chit-CA spectrum (Fig. 5a). In this case a new band at 957 cm^{-1} was detected in the film spectrum. According with the literature, ChCl presents peaks connected with the CH_3 bending and rocking modes as well as to the CH_2 scissoring, wagging, twisting and rocking modes in the wavelength region of 1500–960 cm^{-1}.[28] More, other bands corresponding to the N–C stretching modes from 949 to 707 cm^{-1} were also reported for ChCl spectrum.[28] The absorption band of glucosidic linkage was also observed at 897 cm^{-1} in the Chit-ChCl-CA spectrum. The two films show spectral differences from the chitosan spectrum in the region between 800-700 cm^{-1}. This could suggests the formation of compounds resulting from the Maillard reaction occurring during film processing at 120 ºC.[29]

According to the literature it is possible to distinguish protonated carboxylic groups of citric acid from cross-linked groups that overlap in the FTIR spectrum.[20] By exchanging the counterion of protonated carboxylic acid from protons to Na^+ it is possible to cause a band shift from 1700 cm^{-1} to 1500 cm^{-1} permitting the distinction between free carboxylic acids from ester groups and the quantification of cross-linking effect.[20] In our case, a small shoulder observed in the Chit-ChCl-CA film at 1711 cm^{-1} disappeared and two new bands at 1650 and 1587 cm^{-1} were observed after NaOH treatment (Fig. 5b). In the case of Chit-CA film the shoulder at 1711 cm^{-1} also disappeared after NaOH treatment but any other significant band effect was detected in the Chit-CA film spectrum (Fig. 5b). In light of the previous results films' characteristics could not be only ascribed to cross-linking effects as it was not possible to calculate the band intensity ratio as it was previously reported.[20] According with FTIR information it is possible to say that the changes observed for both film conditions could be associated to the interaction of the different components (acetic acid, ChCl, CA) with the chitosan and by film processing conditions.

Thermogravimetric analysis (TGA)

The thermal stability of processed films Chit-ChCl-CA and Chit-CA was compared with each film component used for their preparation: chitosan powder, citric acid and choline chloride (Fig. 6). Fig. 6a shows the temperature dependence of the relative weight loss (TG curves), while the inset to the figure presents the temperature dependence of the weight loss first derivative (DTG curves) (Fig. 6b).

All samples but CA and ChCl powders showed a significant loss of water during the equilibrium step performed at 60 ºC. In particular, data suggests that Chit-ChCl-CA absorbed more water than Chit-CA, which is consistent with water sorption analysis. Chitosan powder shows a stable weight loss up to approximately 250 ^{o}C (see Figs 6a and 6b). This indicates that chitosan chain cleavage likely not occurred during the compression molding of films at 120 ºC. Indeed, thermal degradation of chitosan powder was reported to start at around 310 ^{o}C.[16] The melting points of citric acid and choline chloride are at approximately 153 and 247 ^{o}C, respectively.[30,31] Overall, the TGA curves of Chit-ChCl-CA and Chit-CA films at lower temperature indicate that the onset of films thermal degradation coincides with the degradation of CA at nearly 200 ºC (Fig 6b). The chitosan thermal degradation in the chitosan film prepared with the eutectic mixture seems to start before chitosan degradation in the powdered sample (Fig. 6a). This observation is consistent with the literature where plasticized chitosan samples presented faster thermal degradation than unplasticized samples.[16]

Films thickness, mechanical and optical properties

The thickness, mechanical and optical properties of Chit-ChCl-CA and Chit-CA films prepared at the optimum conditions are presented in Table 2. In general, films prepared with Chit-ChCl-CA were thicker than Chit-CA films. This observation was confirmed with the SEM images (Figs. 2D and 2E).

With the addition of a plasticizer agent it is expected an alteration in the mechanical properties of the film, namely a reduction in the stress of the material and an increase in the elongation at break. In this case, higher values of *TS* and *YM* were observed for Chit-CA films in relation to films prepared with Chit-ChCl-CA (Table 2). The *TS* value reported here for Chit-CA films corresponds to the value of *TS* found for pure chitosan films.[7] The chemical structure of citric acid (CA) with one hydroxyl and three carboxyl groups (Fig. 1) confers it different functionalities permitting it to act as cross linker or plasticizer agent.[32] In this study it is possible that the CA multi-carboxyl structure serves as cross-linking agent and reinforces the intermolecular binding by introducing covalent bonds that supplement natural intermolecular hydrogen bonds

making the Chit-CA films more rigid (more brittle material). On the other hand, *TS* value obtained for Chit-ChCl-CA are comparable with *TS* values obtained from chitosan plasticized films with glycerol and with ethylene glycol.[7]

To quantify the films' stretch ability when subjected to a given stress we measured the elongation at break, *E*, of the films. As seen in Table 2, films prepared with Chit-ChCl-CA presented higher *E* values when compared with Chit-CA films. The *E* values reported here for the two film formulations are lower than the values obtained from plasticized chitosan films reported in the literature.[7] In this case, CA certainly contributes to the stress-strain behavior of the thermo-compressed films. On the other hand, ChCl combined with CA clearly led to more flexible films. Note that the larger residual water content inherent to the Chit-ChCl-CA film (see Fig. 4) might directly contribute to the *E* characteristic rather than the eutectic mixture itself.

In relation to the films color it is expected that color changes take place during the thermo-compression molding of chitosan films as non-enzymatic browning reactions, Maillard reactions, can be promoted by the high processing temperature and pressure force.[33]

Significant differences were observed for both color parameters: Delta *E* and Opacity between the two film conditions (Table 2). Delta *E* value of Chit-ChCl-CA films was significantly higher when compared with the Delta E value of Chit-CA films. It was reported that Delta *E* of chitosan casting films followed an increasing trend in the same manner as the yellowing index after microwave heating, indicating that yellow color increased due heating.[34] In terms of opacity it is possible to observe that Chit-ChCl-CA film presented higher opacity value than Chit-CA film. The higher opacity observed in Chit-ChCl-CA films could be related to the higher thickness values determined (Table 2).

Conclusions

Deep Eutectic mixture of choline chloride and citric acid (1:1) was successfully used as biodegradable plasticizers for the preparation of chitosan films by thermo-compression molding. The plasticizing capacity of the selected eutectic mixture, at the optimum processing condition, was compared vs. films prepared using just citric acid in their composition.

The mechanical, water resistance, microstructure, optical and thermal properties of the chitosan eutectic mixture films were significantly different from those using just citric acid. Brittle structure of chitosan-CA films was improved by ChCl incorporation in the mixture resulting in less elastic films but with improved elongation at break. This observation is supported by FTIR results even that cross-linking effects could not be

quantified for films formulations. The results presented here shows that chitosan and Deep Eutectic mixture (ChCl-CA) are extremely promising materials for tailoring biofilm design.

For the purpose of specific practical applications of the films produced here, ChCl and CA could need to be removed. Since CA and ChCl removal might affect the final film properties, a detailed investigation of the impact of such removal will be performed in the future.

Acknowledgements

This work was supported by the European Union (FEDER) and National funds from the National Strategic Reference Framework Portugal 2007-2013 (QREN) allocated through the Operational Competitiveness Program (COMPETE) and the North Portugal Regional Operational Program (ON.2) (FCOMP-01-0124-FEDER-37285, FCOMP-01-0124-FEDER-041438, NORTE-07-0124-FEDER-000069, NORTE-07-0124-FEDER-000037) to REQUIMTE and I3N through the Portuguese Foundation for Science and Technology (FCT) (projects: UID/QUI/50006/2013, PEst-C/CTM/LA0025/2011, and exploratory project EXPL/QEQ-QFI/0368/2013).

Notes and references

1 N. Peelman, P. Ragaert, B. De Meulenaer, D. Adons, R. Peeters, L. Cardon, F. Van Impe and F. Devlieghere, *Trends Food Sci. Technol.*, 2013, **32**, 128–141.

2 S. Mina, M. Miya, R. Iwamoto and S. Yoshikawa, *J. Appl. Polym. Sci.*, 1983, **28**, 1909–1917.

3 K. Nadaraj, W. Prinyawiwatkul, H. K. No, S. Sathivel and Z. Xu, *J. Food Sci.*, 2006, **71**, E33–E39.

4 A. F. Nikolaev, A. A. Prokopov, E. S. Shulgina and M. V. Vinogradov, *J. Appl. Chem. USSR*, 1987, **60**, 209–210.

5 V. Epure, M. Griffon, E. Pollet and L. Avérous, *Carbohydr. Polym.*, 2011, **83**, 947–952.

6 H. K. S. Souza, J. M. Campiña, A. M. M. Sousa, F. Silva and M. P. Gonçalves, *Food Hydrocoll.*, 2013, **31**, 227–236.

7 N. E. Suyatma, L. Tighzert, A. Copinet and V. Coma, *J. Agric. Food Chem.*, 2005, **53**, 3950–3957.

8 Y. Dai, J. Van Spronsen, G. J. Witkamp, R. Verpoorte and Y. H. Choi, *J. Nat. Prod.*, 2013, **76**, 2162–2173.

9 Y. Dai, J. van Spronsen, G. J. Witkamp, R. Verpoorte and Y. H. Choi, *Anal. Chim. Acta*, 2013, **766**, 61–68.

10 Q. Zhang, K. De Oliveira Vigier, S. Royer and F. Jérôme, *Chem. Soc. Rev.*, 2012, **41**, 7108–7146.

11 A. P. Abbott, A. D. Ballantyne, J. P. Conde, K. S. Ryder and W. R. Wise, 2012, **14**, 1302–1307.

12 E. Leroy, P. Decaen, P. Jacquet, G. Coativy, B. Pontoire, A.-L. Reguerre and D. Lourdin, *Green Chem.*, 2012, **14**, 3063–3066.

13 A. A. Shamsuri and R. Daik, *Bioresources*, 2012, **7**, 4760–4775.

14 A. M. M. Sousa, H. K. S. Souza, N. Latona, C. K. Liu, M. P. Gonçalves and L. Liu, *Carbohydr. Polym.*, 2014, **111**, 206–214.

15 H. K. S. Souza, G. Bai, M. P. Gonçalves and M. Bastos, *Thermochim. Acta*, 2009, **495**, 108–114.

16 M. Matet, M. C. Heuzey, E. Pollet, A. Ajji and L. Avérous, *Carbohydr. Polym.*, 2013, **95**, 241–251.

17 D. C. Montgomery, in *Design and Analysis of Experiments*, John Wiley & Sons, Inc., Canada, 3rd edn., 1991, pp. 521–563.

18 F. D. S. Larotonda, PH.D. Thesis, Univesity of Porto, 2007.

19 ASTM E96-00, 2000.

20 M. H. Pamela de Cuadro, Tiina Belt, Katri S. Kontturi, Mehedi Reza, Eero Kontturi, Tapani Vuorinen, *React. Funct. Polym.*, 2015, **90**, 21–24.

21 C. A. Kienzle-Sterzer, D. Rodriguez-Sanchez and C. Rha, *Makromol. Chem*, 1982, **183**, 1353–1359.

22 F. S. Kittur, A. B. Vishu Kumar and R. N. Tharanathan, *Carbohydr. Res.*, 2003, **338**, 1283–1290.

23 K. Sakurai, *Polymer (Guildf).*, 2000, **41**, 7051–7056.

24 M. K. Cheung, K. P. Y. Wan and P. H. Yu, *J. Appl. Polym. Sci.*, 2002, **86**, 1253–1258.

25 S. Y. Park, K. S. Marsh and J. W. Rhim, *J. Food Sci.*, 2002, **67**, 194–197.

26 M. R. Kasaai, *Carbohydr. Polym.*, 2008, **71**, 497–508.

27 M. Ibrahim and E. Koglin, *Acta Chim. Slov.*, 2004, **51**, 453–460.

28 A. Pawlukojć and Ł. Hetmańczyk, *Chem. Phys.*, 2014, **445**, 31–37.

29 K. Umemura and S. Kawai, *J. Appl. Polym. Sci.*, 2008, **108**, 2481–2487.

30 M. F. Cervera, J. Heinämäki, N. de la Paz, O. López, S. L. Maunu, T. Virtanen, T. Hatanpää, O. Antikainen, A. Nogueira, J. Fundora and J. Yliruusi, *AAPS PharmSciTech*, 2011, **12**, 637–649.

31 H. Mąka, T. Spychaj and K. Kowalczyk, *J. Appl. Polym. Sci.*, 2014, **40401**, 1–7.

32 R. Shi, J. Bi, Z. Zhang, A. Zhu, D. Chen, X. Zhou, L. Zhang and W. Tian, *Carbohydr. Polym.*, 2008, **74**, 763–770.

33 O. Lopez, M. A. Garcia, M. A. Villar, A. Gentili, M. S. Rodriguez and L. Albertengo, *LWT - Food Sci. Technol.*, 2014, **57**, 106–115.

34 C. Jacquot, M. Jacquot, P. Marques, J. Jasniewski, M. J. Akhtar, A. S. Dedelot and S. Desobry, *J. Appl. Polym. Sci.*, 2014, **131**, 9365–9372.

677 **Table 1** GAB parameters (obtained from fitting of sorption isotherms experimental data
678 from Eq. (1)) and water vapor permeability (WVP) for the Chit-ChCl-CA and Chit-CA
679 films prepared by thermo-compression molding using optimum conditions

	C	X_o	k	R^2	WVP x 10^{-10} (g· m^{-1}· s^{-1} ·Pa^{-1})
Chit-CA	6.15	0.003	0.91	0.981	0.85 ± 0.01
Chit-ChCl-CA	6.65	0.002	1.01	0.994	2.87 ± 0.16

680
681
682
683
684
685
686
687
688
689
690
691
692
693
694
695
696
697
698
699
700
701

Table 2 Film thickness (d), mechanical properties (tensile strength, TS; elongation at break, E; and Young´s modulus, YM), and color parameters (Delta E and opacity) of the Chit-ChCl-CA and Chit-CA films prepared by thermo-compression molding using optimum conditions*

	d (mm)	*TS* (MPa)	*E* (%)	*YM* 10^2 (MPa)	Delta *E*	Opacity (%)
Chit-CA	0.038 ± 0.004[b]	63.8 ± 10.3[b]	3.0 ± 0.6[b]	37.0 ± 8.6[b]	19.2 ± 1.71[b]	13.2 ± 0.41[b]
Chit-ChCl-CA	0.042 ± 0.005[a]	28.0 ± 7.4[a]	4.5 ± 0.8[a]	20.5 ± 3.6[a]	22.0 ± 1.34[a]	13.9 ± 0.72[a]

*Means in the same column with different letter are significantly different ($p < 0.05$)

727 **Figure Captions.**

728 **Fig. 1** Chemical structure representation of chitosan, choline chloride and citric acid.
729 Mixture appearance of the three components for film production.

730 **Fig. 2** Representative SEM pictures of the surface of films at 150x magnification (A —
731 Chit-ChCl-CA and B — Chit-CA), of the cross-sections of cryo fractured films at 1000x
732 magnification (D — Chit-ChCl-CA and E — Chit-CA) and of Chit-ChCl-CA films
733 prepared without acetic acid of surface at 150x (C) and of cross-sections at 250x (F).

734 **Fig. 3** DSC thermograms of Chit-ChCl-CA and Chit-CA films obtained from first heating
735 run (a) and from second heating run (b).

736 **Fig. 4** Experimental sorption data (i.e. equilibrium moisture content, *Xe* vs. water
737 activity, a_W) and respective fit using the GAB model (Eq. (2)) for the Chit-ChCl-CA film
738 (■) and for the Chit-CA film (●).

739 **Fig. 5** FTIR spectra of Chit-ChCl-CA film, Chit-CA film, and Chit powder (spectral range
740 from 4000 to 600 cm^{-1}) (a). Spectra of Chit-ChCl-CA and Chit-CA films before and after
741 NaOH immersion treatment (spectral range from 2000 to 600 cm^{-1}) (b).

742 **Fig. 6** TG (a) and DTG (b) curves of Chit-ChCl-CA film, Chit-CA film, chit powder, CA
743 powder and ChCl.

744

745

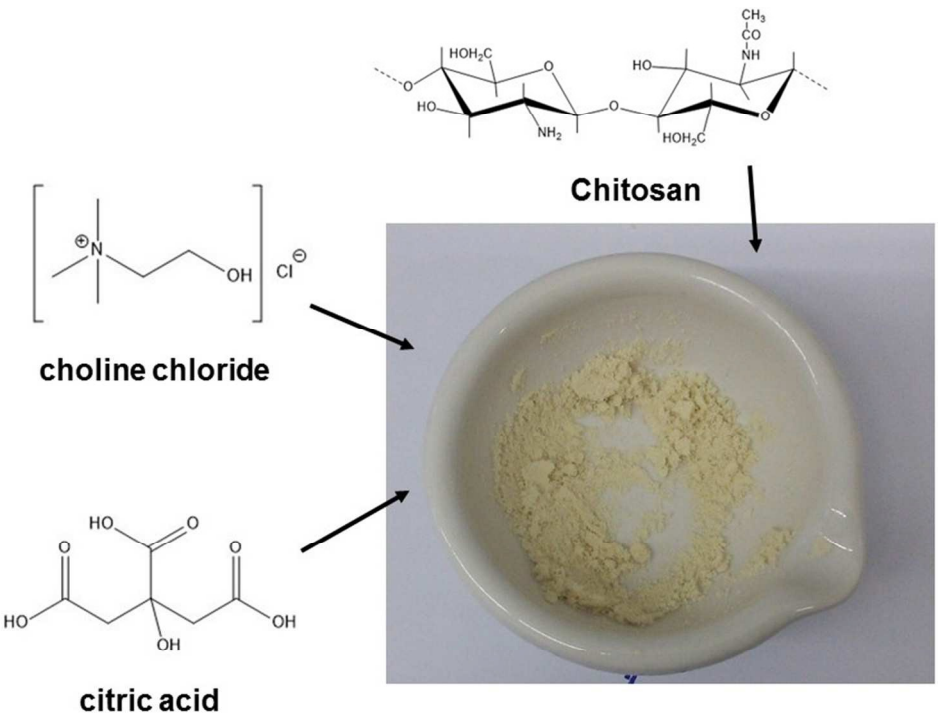

237x177mm (96 x 96 DPI)

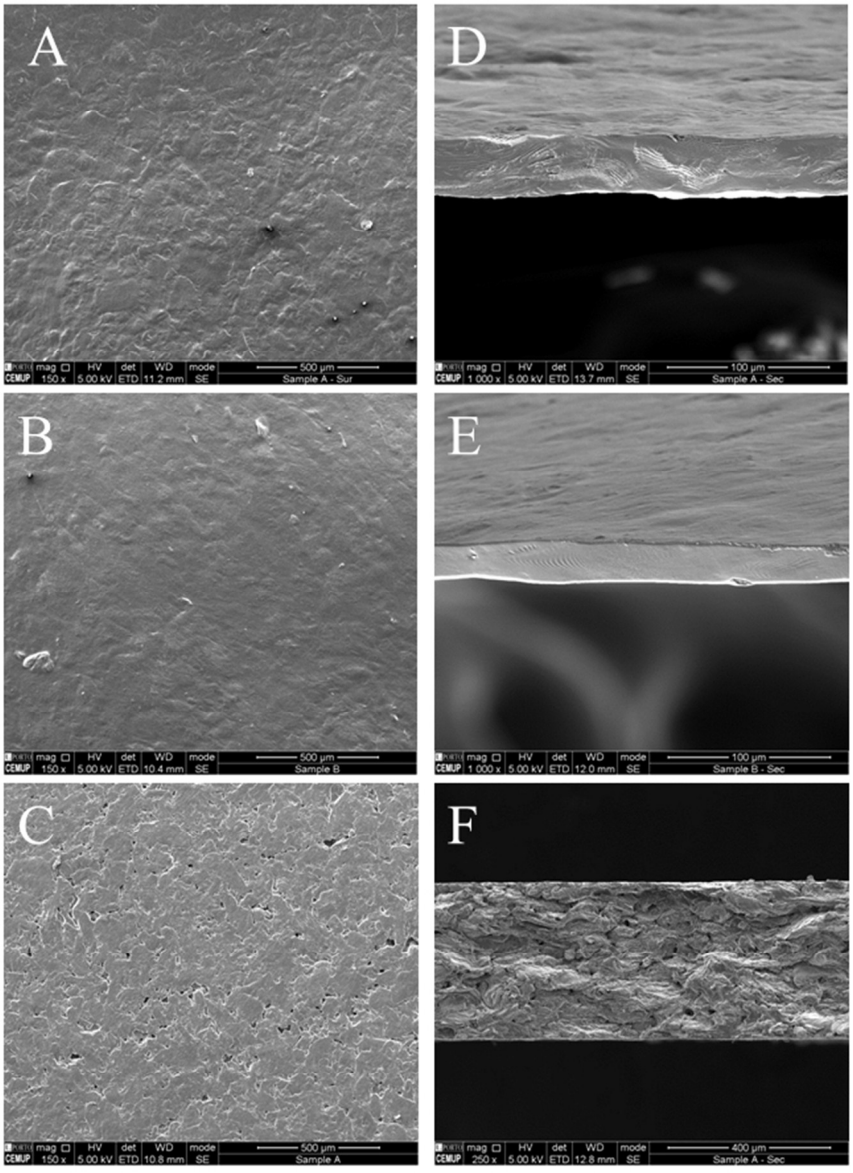

175x240mm (96 x 96 DPI)

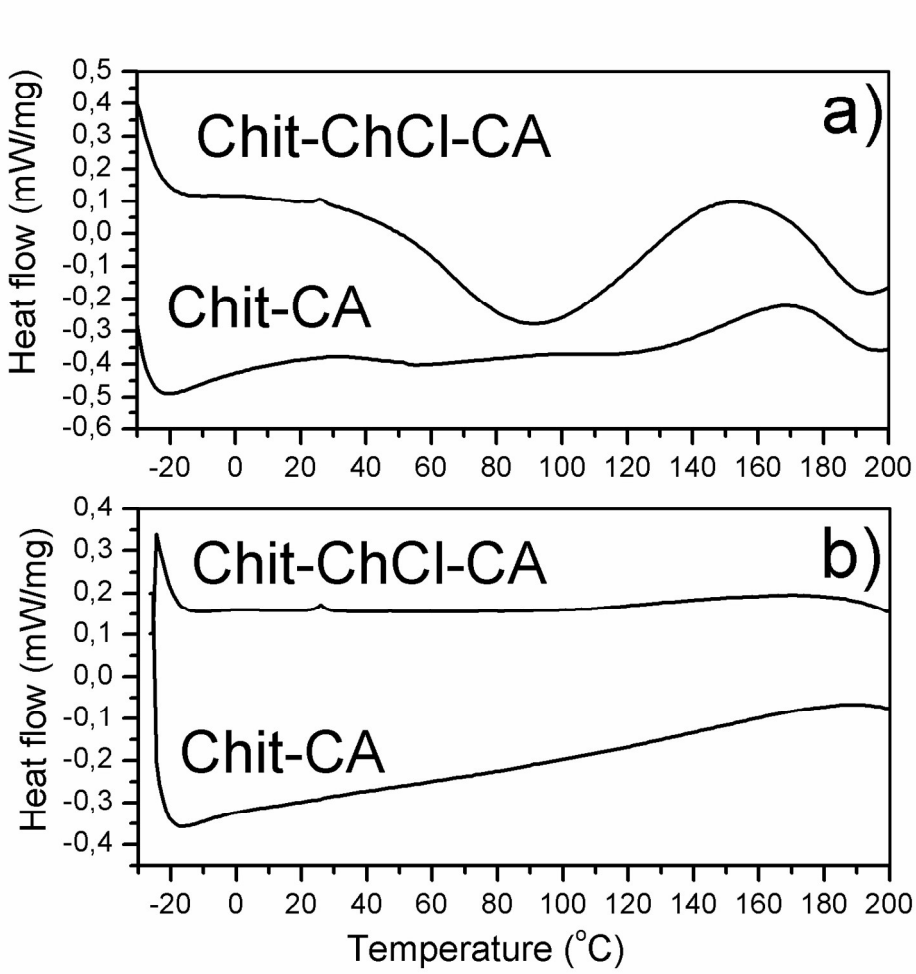

281x287mm (150 x 150 DPI)

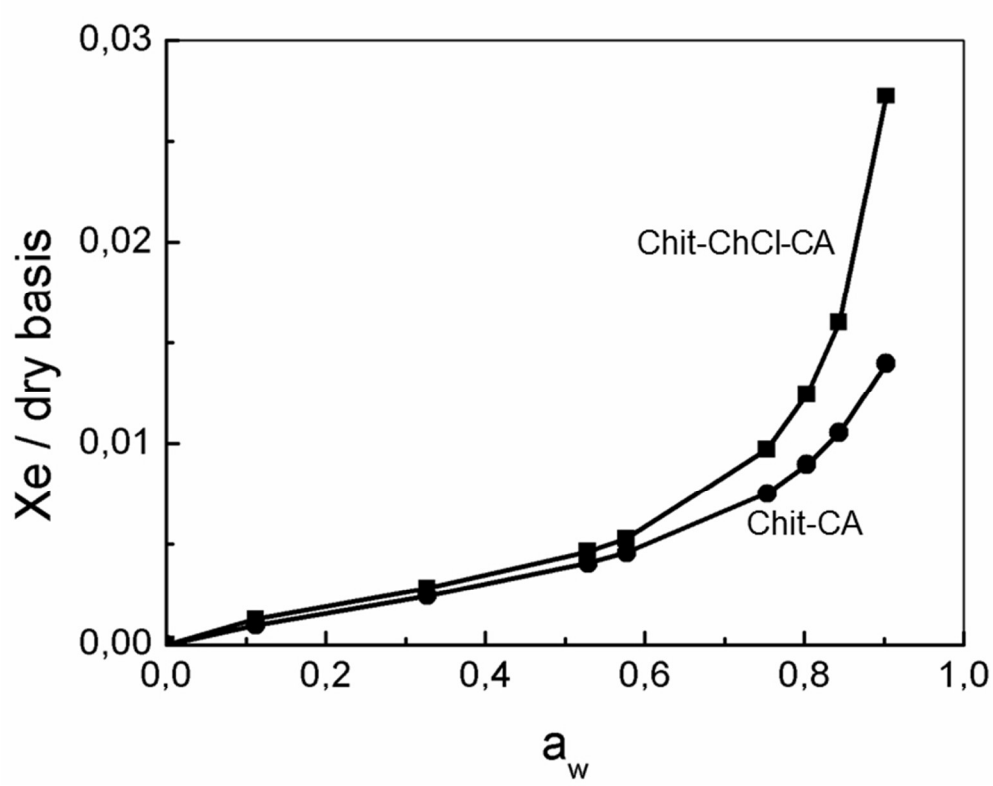

217x171mm (96 x 96 DPI)

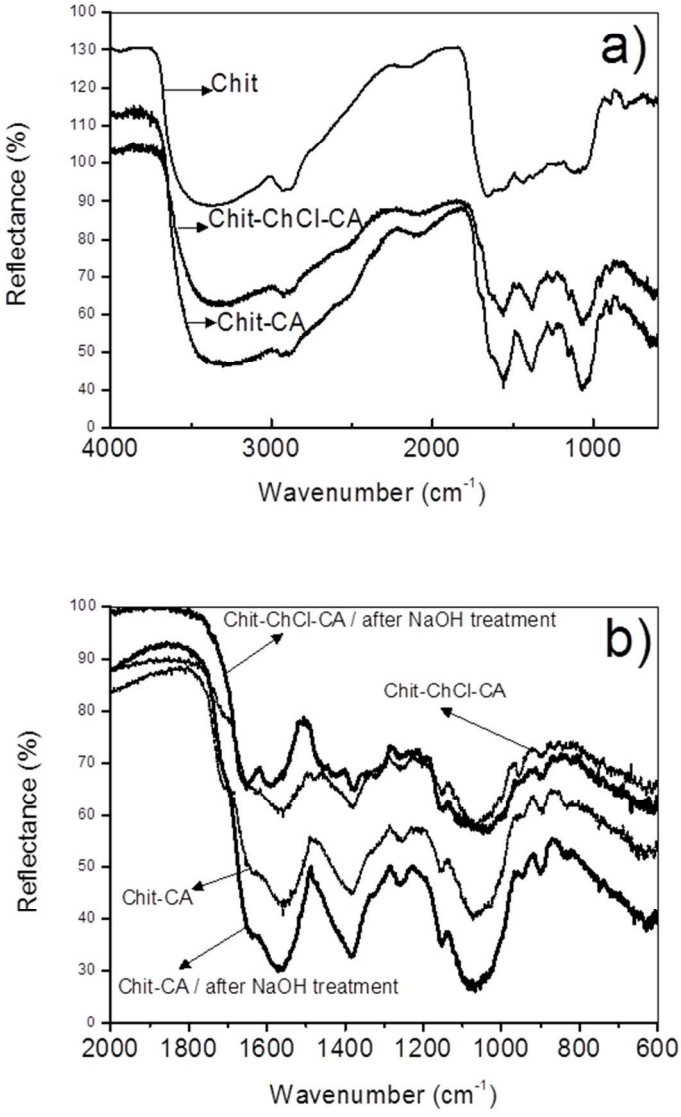

190x254mm (96 x 96 DPI)

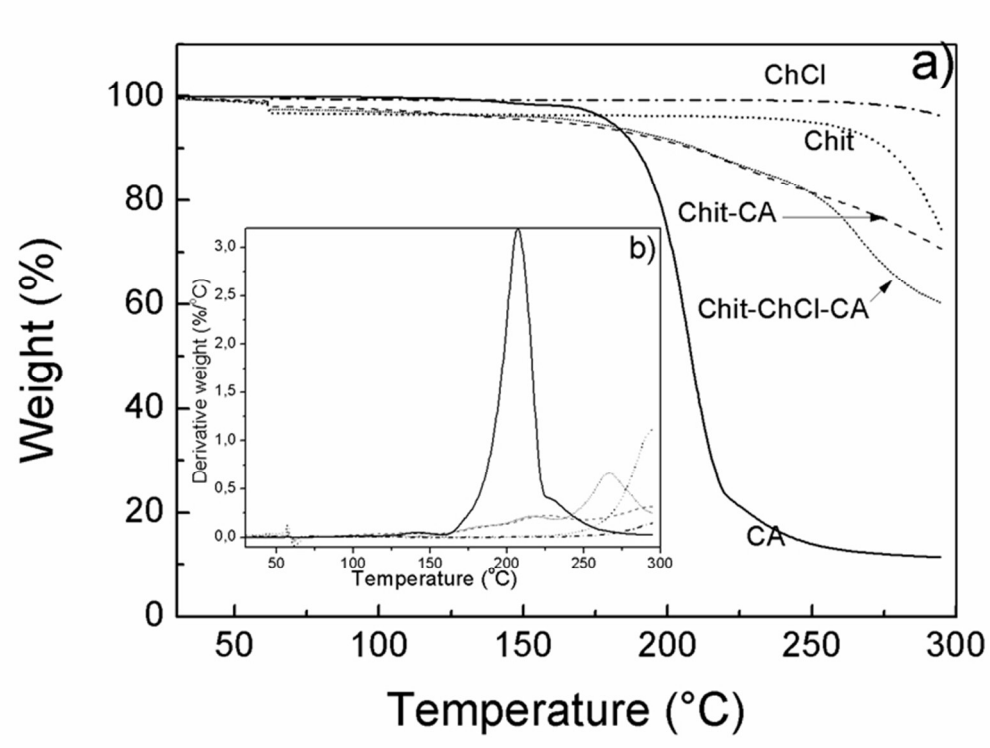

222x170mm (96 x 96 DPI)

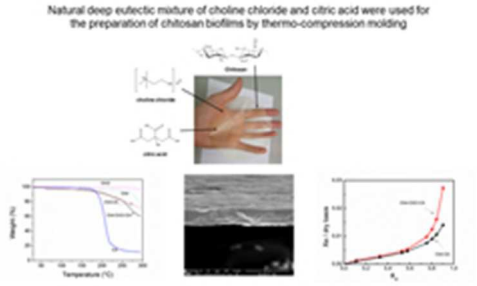

70x39mm (96 x 96 DPI)

Electronic Supplementary Information

Thermo-compression molding of chitosan with deep eutectic mixture for biofilms development

Andrea C. Galvis-Sánchez[a,*], *Ana M. M. Sousa*[a,b], *Loic Hilliou*[c], *Maria P. Gonçalves*[a], *Hiléia K.S. Souza*[a,*]

[a] REQUIMTE/LAQV, Departamento de Engenharia Química, Faculdade de Engenharia, Universidade do Porto, Rua Dr. Roberto Frias, 4200-465 Porto, Portugal.

[b] Agricultural Research Service, U.S. Department of Agriculture, Eastern Regional Research Center, Dairy & Functional Foods Research Unit, 600 East Mermaid Lane, Wyndmoor, PA 19038, USA.

[c] Institute for Polymers and Composites/I3N, University of Minho, Campus de Azurém, 4800-058 Guimarães, Portugal.

Corresponding Authors:

*Andrea C. Galvis-Sánchez (Phone: +351 220414838; E-mail address: asanchez@fe.up.pt); Hiléia K. S. Souza (Phone: +351 220414838; E-mail address: hsouza@fe.up.pt)

ESI 1. Materials ad Methods

ESI 1.1 Optimization strategy

The Box-Behnken design (BBD) with response surface methodology (RSM) were used to find the conditions of eutectic mixture amount (X_1; %), compression load (X_2; kN) and compression time (X_3; min) that ensured films with lower energy requirements and best mechanical properties consisted in 12 experimental runs (runs 1-12 in Table S1) with three levels for each factor (high, intermediate and low values coded as +1, 0 and -1, respectively) plus 3 replications at the center point (all factors at 0 level; runs 13-15 in Table S1).[17]

The tensile strength, *TS* (Y_1; MPa) and elongation at break, *E* (Y_2; %) of the chitosan films obtained in each experimental run (Table S1) were fitted to second order models to obtain the optimal conditions for film production by multifactor variance analysis (ANOVA) and inspection of 3D response surface plots. Statistical significance was determined by student's *t*-test and *p*-values for a 95% confidence level ($p<0.05$). All analyses were performed using the *Statistica 8.0* software (StatSoft, Tulsa, OK, USA).

ESI 1.2 Wide Angle X-ray diffraction (WAXD)

WAXD spectra of optimized films samples were acquired at room temperature with a Bruker D8 Discover diffractometer (lambda source of 0.154 nm). Film samples were scanned at diffraction angles (2θ) from 5 to 35o using 0.04º steps. Chitosan powder with no further preparation was also analyzed with the same procedure (Fig S2).

ESI 2. Results and discussion

ESI 2.1 Optimal conditions for film production

The experimental domain and independent variables affecting the TS and E of the films were chosen after preliminary single-factor experiments (data not shown). The use of BBD avoided getting experimental points at extreme values of the design space[17] and this was important for the eutectic mixture amount and applied load which were very hard to use outside the ranges listed in Table S1 (20-40% and 176.5-215.7 kN, respectively).

As desired, the *TS* and *E* regression models reached high statistical significance ($p<0.003$) while their lack of fit was not significant ($p>0.05$; Table S2). The significant effect of the factors on the studied responses was confirmed by the high F-values obtained for both models (12.62 and 10.34, respectively; Table S2). The correlation (R^2) and adjusted correlation (R^2-adj) coefficients of the models were high and as close as 0.9044 and 0.8327 for *TS* and 0.8858 and 0.8002 for *E* confirming a

good agreement between predicted and observed data. Based on this information both regression equations were considered adequate[17] and optimal conditions for film production were found by ANOVA analysis and 3D surface plots inspection (Figs. S1a, b).

The amount of eutectic mixture in the film (X1) was the most influential effect ($p<0.0002$; Table S2) for TS. Films with less eutectic mixture (20%) showed higher mechanical strength than those prepared with more (40%; respectively, runs 1 vs 2, 3 vs 4, 5 vs 6 and 7 vs 8 in Table S1). Improved mechanical strength was found when using 20% eutectics and high or low compression loads (215.7 or 176.5 kN; not shown) as well as long or short compression times (10 or 20 min; Fig. S1a). This agreed well with the strong curvature affecting the TS surface profile imposed by the applied load (X22; $p<0.05$) and compression time (X32; $p<0.002$). Considering energy and time savings, best possible set of conditions for maximum TS could be (set1): 20% of plasticizer, 176.5 kN of applied load and 15 min of compression time. Experimental runs producing the most resistant films (TS ~ 46-48 MPa; Table S1), i.e. run 9 (set2: 30% eutectic mixture, 176.5 kN, 10 min) and run 10 (set3: 30% eutectic mixture, 215.7 kN, 10 min) were also tested and no significant differences ($p> 0.05$) were found between the three sets of conditions after means comparison using the Student's t-test.

The compression time was not an influential parameter to *E* ($p>0.05$; Table S2) contrarily to the applied load, X_2 ($p<0.005$; Table S2), and the quadratic effect of the eutectic mixture amount, X_1^2 ($p<0.0002$). Films prepared using low compression load (176.5 kN) showed higher *E* (Fig. S1b) (e.g. runs 9 and 11; Table S1). Formulations with 30% eutectic mixture processed at 176.5 kN led to films with higher *E* than those prepared with 40% (Fig. S1b). This agreed well with a previous study where an increase in plasticizer content led to a drastic reduction in the mechanical properties, *TS* and E, of compression molded chitosan films.[16] The authors attributed that phenomenon to a phase separation that can occur between the polyol and the chitosan polysaccharide. Unfortunately, in our case the phase separation hypothesis was not fully supported by structural information.

Our highest *E* was obtained in run 9 (~4.19%; Table S1) set of conditions (set2: 30% plasticizer, 176.5 kN, 10 min) was chosen as optimal for film production.

Table S1 Real and coded values for the three-level-three-factor Box-Behnken design (X_1 – % of eutectic mixture; X_2 – applied load; X_3 – time) and experimental results for the response variables, tensile strength, *TS* (Y_1; MPa) and elongation at break, *E* (Y_2; %). Values of Y_1 and Y_2 for each run represent a mean of three replicates

	Real values			Response	
Run	X_1 (%)	X_2 (kN)	X_3 (min)	Y_1 (MPa)	Y_2 (%)
1	20 (-)	176.5 (-)	15 (0)	39.6	1.87
2	40 (+)	176.5 (-)	15 (0)	30.0	1.30
3	20 (-)	215.7 (+)	15 (0)	42.0	0.89
4	40 (+)	215.7 (+)	15 (0)	21.9	1.23
5	20 (-)	196.1 (0)	10 (-)	43.8	1.38
6	40 (+)	196.1 (0)	10 (-)	26.7	1.24
7	20 (-)	196.1 (0)	20 (+)	43.5	1.09
8	40 (+)	196.1 (0)	20 (+)	32.2	1.56
9	30 (0)	176.5 (-)	10 (-)	46.4	4.19
10	30 (0)	215.7 (+)	10 (-)	48.6	2.03
11	30 (0)	176.5 (-)	20 (+)	38.8	3.69
12	30 (0)	215.7 (+)	20 (+)	43.5	2.25
13	30 (0)	196.1 (0)	15 (0)	39.7	2.12
14	30 (0)	196.1 (0)	15 (0)	36.0	2.69
15	30 (0)	196.1 (0)	15 (0)	34.7	2.92

Table S2 Analysis of variance (ANOVA) for the regression models excluding non-significant interactions X_iX_j.

Response	Source	SS	DF	MS	F-value	P
TS (Y_1; MPa)	Model	847.8	6	141.3	12.62	0.00107[a]
	X_1	468.2	1		41.80	<0.0002[a]
	X_2	1.36	1	1.36	0.1215	0.7364[b]
	X_3	7.03	1		0.6278	0.4510[b]
	X_1^2	46.17	1		4.033	0.0795[b]
	X_2^2	67.6	1	67.6	6.03	0.0396[a]
	X_3^2	249.9	1	249.9	22.32	<0.00149[a]
	Residual	89.60	8	11.20		
	Lack of fit	83.87	6	13.98	4.875	0.1799[b]
	Pure error	5.73	2	2.87	49.28	0.02001[a]
	Total	937.4	14			
	R^2	0.9044				
	R^2-adj	0.8327				
E (Y_2; %)	Model	11.714	6	1.9523	10.34	0.00211[a]
	X_1	0.02531	1	0.02531	0.1314	0.7237[b]
	X_2	2.856	1	2.856	15.13	0.00461[a]
	X_3	0.01361	1	0.01361	0.07212	0.7951[b]
	X_1^2	7.974	1	7.974	42.25	0.000188[a]
	X_2^2	0.2955	1	0.2955	1.566	0.2462[b]
	X_3^2	0.1202	1	0.1202	0.6368	0.4479[b]
	Residual	1.50997	8	0.18875		
	Lack of fit	1.1707	6	0.19512	1.15022	0.5339[b]
	Pure error	0.3393	2	0.1696	11.509	0.08209[b]
	Total	13.224				
	R^2	0.8858				
	R^2-adj	0.8002				

SS= Sum of squares; DF= Degree of freedom; MS= Mean square; R^2= quadratic correlation coefficient; R^2-adj= adjusted quadratic correlation coefficient; [a] significant ($p<0.05$); [b] not significant ($p>0.05$)

Figure S1 a) 3D response surface plot of tensile strength (*TS*) of chitosan films (Y_1) as a function of eutectic mixture % (X_1) and time (X_3) (compression load (X_2) = 196.1 kN).

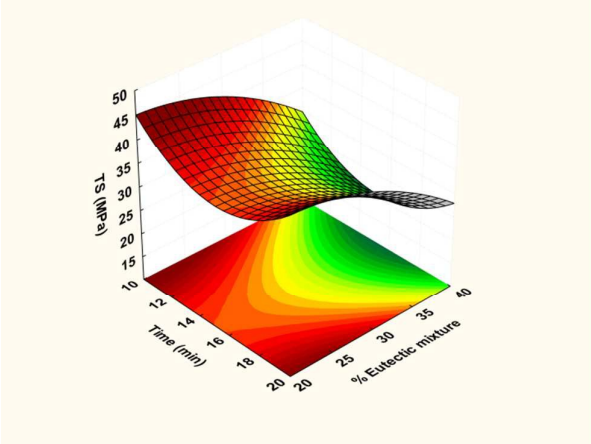

Figure S1 b) 3D response surface plot of elongation at break, (*E*) of chitosan films (Y_2) as a function of eutectic mixture % (X_1) and compression load (X_2) (time (X_3) = 15 min).

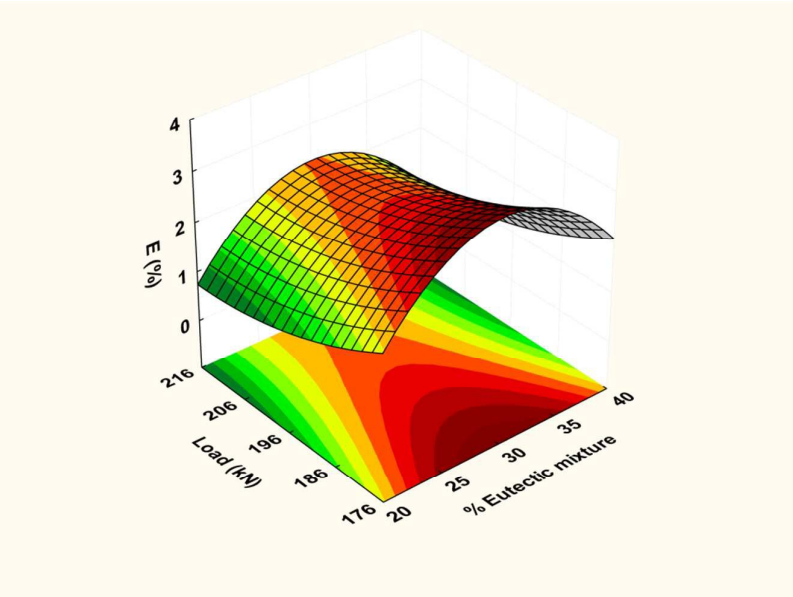

Fig. S2 XRD spectra of chitosan powder, and thermo-compressed Chit-CA and Chit-ChCl-CA films.